Biomaterials 33 (2012) 4515–4525

Contents lists available at SciVerse ScienceDirect

Biomaterials

journal homepage: www.elsevier.com/locate/biomaterials

Highly efficient magnetic stem cell labeling with citrate-coated superparamagnetic iron oxide nanoparticles for MRI tracking

Kristin Andreas [a,*], Radostina Georgieva [b], Mechthild Ladwig [c], Susanne Mueller [d], Michael Notter [e], Michael Sittinger [a], Jochen Ringe [a]

[a] Tissue Engineering Laboratory and Berlin-Brandenburg Center for Regenerative Therapies, Department of Rheumatology and Clinical Immunology, Charité-Universitätsmedizin Berlin, Charitéplatz 1, 10117 Berlin, Germany
[b] Institute of Transfusion Medicine and Berlin-Brandenburg Center for Regenerative Therapies, Charité-Universitätsmedizin Berlin, Charitéplatz 1, 10117 Berlin, Germany
[c] Institute of Vegetative Physiology, Charité-Universitätsmedizin Berlin, Charitéplatz 1, 10117 Berlin, Germany
[d] Department of Experimental Neurology and Center for Stroke Research Berlin, Charité-Universitätsmedizin Berlin, Charitéplatz 1, 10117 Berlin, Germany
[e] Department of Hematology and Oncology, Charite-Universitätsmedizin Berlin, Hindenburgdamm 30, 12200 Berlin, Germany

ARTICLE INFO

Article history:
Received 13 February 2012
Accepted 29 February 2012
Available online 24 March 2012

Keywords:
Mesenchymal stem cell
Magnetic cell labeling
Superparamagnetic iron oxide nanoparticles
Magnetic resonance imaging
In vivo cell tracking
Tissue engineering

ABSTRACT

Tracking of transplanted stem cells is essential to monitor safety and efficiency of cell-based therapies. Magnetic resonance imaging (MRI) offers a very sensitive, repetitive and non-invasive *in vivo* detection of magnetically labeled cells but labeling with commercial superparamagnetic iron oxide nanoparticles (SPIONs) is still problematic because of low labeling efficiencies and the need of potentially toxic transfection agents. In this study, new experimental citrate-coated SPIONs and commercial Endorem and Resovist SPIONs were investigated comparatively in terms of *in vitro* labeling efficiency, effects on stem cell functionality and *in vivo* MRI visualization. Efficient labeling of human mesenchymal stem cells (MSCs) without transfection agents was only achieved with Citrate SPIONs. Magnetic labeling of human MSCs did not affect cell proliferation, presentation of typical cell surface marker antigens and differentiation into the adipogenic and osteogenic lineages. However, chondrogenic differentiation and chemotaxis were significantly impaired with increasing SPION incorporation. Transplanted SPION-labeled MSCs were visualized *in vivo* after intramuscular injection in rats by 7T-MRI and were retrieved *ex vivo* by Prussian Blue and immunohistochemical stainings. Though a careful titration of SPION incorporation, cellular function and MRI visualization is essential, Citrate SPIONs are very efficient intracellular magnetic labels for *in vivo* stem cell tracking by MRI.

1. Introduction

Mesenchymal stem cells (MSCs), also called mesenchymal stromal cells, have the potential to migrate after systemic transplantation along chemokine gradients to diseased tissues where they engraft, differentiate into the defective cell type and/or induce regenerative processes through paracrine mechanisms [1–4]. Until now, systemic MSC therapy has been applied to treat various injuries such as stroke, myocardial infarction and bone fractures [3,5–8]. However, crucial to assess the efficiency and safety of such cell-based therapies is to track the transplanted cells *in vivo* in order to monitor cellular biodistribution, engraftment and fate without postmortem histology. In this regards, magnetic resonance imaging (MRI) is an excellent tool for tracking magnetically labeled cells *in vivo* non-invasively, repeatedly and with high spatial resolution. Magnetic cell labeling is typically achieved by adding superparamagnetic iron oxide nanoparticles (SPIONs) to the cultivation medium during *in vitro* cell expansion: the nanoparticles are internalized, accumulated intracellularly and give hypointensities in T2*-weighted MRI [9–12]. Numerous studies already demonstrated the *in vivo* tracking of SPION-labeled MSCs by MRI in various tissues, such as brain, liver, kidney, spinal cord, myocardial heart and traumatic muscle tissue [13–17].

As agents for magnetic cell labeling commercialized SPIONs, in particular dextran-coated Endorem and carboxydextran-coated Resovist, are most commonly used. Nanoparticles of both types are of standard size within the range of 50–200 nm, are easily phagocyted by Kupffer cells of the reticuloendothelial system (RES) upon intravenous administration and are clinically applied for liver and spleen imaging by MRI [11,18]. Because MSCs lack substantial phagocytic capacity only poor intracellular SPION uptake and limited MRI sensitivity are yielded with the commercial nanoparticles

* Corresponding author. Tel.: +49 30 450 513 188; fax: +49 30 450 513 957.
E-mail address: kristin.andreas@charite.de (K. Andreas).

0142-9612/$ – see front matter © 2012 Elsevier Ltd. All rights reserved.
doi:10.1016/j.biomaterials.2012.02.064

[19–21]. Hence, high SPION labeling concentrations in the cultivation medium, the use of potentially toxic transfection agents or complex SPION surface modifications are required to achieve magnetic MSC labeling with commercial SPIONs that is sufficient for *in vivo* tracking by MRI [20,22–24].

A new type of not yet commercialized nanoparticles has emerged: nonpolymer-coated SPIONs that are stabilized with anionic monomers or chelating agents, such as citrate or dimercaptosuccinic acid. Until now, magnetic labeling with small-sized (hydrodynamic diameter < 50 nm) anionic SPIONs has been performed for several cell types, such as macrophages, HeLa cells and fibroblasts yielding high internalization efficiencies [23,25–27]. So far, however, there are no published data on the labeling of any type of stem cell with anionic SPIONs of standard size, the cellular effects of magnetic labeling and the *in vivo* detection by MRI.

In this study, new experimental anionic citrate-coated SPIONs and commercial Endorem and Resovist SPIONs were investigated comparatively for *in vitro* magnetic labeling of human MSCs. We performed type- and dose-dependent cell labeling studies investigating the intracellular iron uptake and the MRI signal loss. Furthermore, the impact of magnetic labeling on mesenchymal stem cell function was determined. Finally, *in vivo* and *ex vivo* visualization of transplanted SPION-labeled MSCs was investigated in rat muscle tissue by MRI and immunohistochemical stainings.

2. Materials and methods

2.1. Synthesis and characterization of SPIONs

Endorem (Guerbet, Sulzbach, Germany) and Resovist (Bayer HealthCare Pharmaceuticals, Berlin, Germany) SPIONs are clinically approved contrast agents that were purchased from the local distributor. Endorem SPIONs are also commercialized with the trade name Feridex outside of Europe. Experimental Citrate SPIONs were prepared by co-precipitation. In brief, an aqueous mixture of 0.05 M $FeCl_2 \times 4H_2O$ and 0.1 M $FeCl_3 \times 6H_2O$ was alkalized with 25% ammonia under moderate stirring at 75 °C for 30 min. Obtained iron oxide nanoparticles were magnetically separated, washed with distilled water and stabilized using hydrochloric acid. Subsequently, nanoparticles were complexed by adding citric acid under constant stirring at 50 °C for 30 min. Finally, SPIONs were magnetically separated, washed with distilled water and the pH value was adjusted to 7.5 by slowly adding sodium hydroxide.

The hydrodynamic particle diameter of the three SPION types was measured by dynamic light scattering and the zeta potential was determined by laser Doppler velocimetry (ZetaSizer nano ZS, Malvern Instruments, Worcestershire, UK). The particle size measurements were performed in distilled water, 1.5 mM NaCl and 150 mM NaCl. Zeta potential was measured in 150 mM NaCl. Results are shown as means ± standard deviation ($n = 5$). The iron oxide core size of Citrate SPIONs was determined from transmission electron micrographs (TEM, EM 912 Ω; Zeiss MicroImaging, Jena, Germany).

2.2. Magnetic cell labeling

Human MSCs were isolated from iliac crest bone marrow aspirates from normal donors and cultivated as described previously [28,29]. The bone marrow aspirates were received in accordance with the local ethical committee. For dose-dependent studies magnetic labeling of human MSCs was performed at passage three by incubation of adherent cells with various concentrations of Resovist (25–1000 μg Fe/ml), Endorem (25–2000 μg Fe/ml) and Citrate (5–100 μg Fe/ml) SPIONs in the cultivation medium. Chosen concentration ranges resulted from preliminary experiments (data not shown). Note that no transfection agent was used. After 24 h, labeled adherent MSCs were repeatedly washed with phosphate-buffered saline (PBS; Biochrom) to remove excess SPIONs, trypsinized and washed again three times with PBS prior to further investigations. To determine the effect of magnetic labeling on the function of MSCs, cells were labeled with 25 μg Fe/ml Citrate SPIONs and 500 μg Fe/ml Endorem SPIONs, respectively, and characterized comparatively to unlabeled cells.

2.3. Intracellular iron quantification

To quantify the intracellular iron content, 0.5×10^6 labeled MSCs were lysed in 5 ml 20% hydrochloric acid and analyzed for iron using inductively coupled plasma optical emission spectrometry (ICP-OES; JY 38 Plus, Jobin-Yvon ISA, France). Three replicates were measured for three individual donors and results are shown as means ± standard deviation.

2.4. In vitro MRI of cell phantoms

MRI was performed with a 7 T rodent scanner (PharmaScan 70/16, Bruker BioSpin, Rheinstetten, Germany) operating with Bruker software Paravision 4.0. For MR imaging a linear 1H-RF – volume resonator with an inner diameter of 38 mm was used. One million MSCs labeled with Resovist, Endorem and Citrate SPIONs at increasing concentrations were embedded into 2 ml 3% (w/v) agarose. T2*-weighted imaging was performed using a 2D-gradient-echo sequence (FLASH) with TR/TE = 619.7/7.2 ms, flip angle 30° and 4 averages for 15 axial slices and a slice thickness of 1.0 mm, a FOV of 30 × 30 mm and a matrix size of 256 × 256. MRI data evaluation of cell phantoms was carried out with Analyze 5.0 software (AnalyzeDirect, Inc., Lenexa USA). Signal decrease of SPION-labeled MSCs was determined by ROI-analysis for three individual donors ($n = 3$). The mean signal intensity of cell phantoms was determined over 10 slices, the signal-to-noise ratios (SNR) were calculated and normalized to the SNR of the unlabeled controls.

2.5. Prussian Blue staining

Prussian Blue staining was performed to visualize intracellular SPIONs. Very briefly, fixated cells were incubated for 30 min in a mixture of 2% potassium ferrocyanide and 2% hydrochloric acid at equal volumes and counterstained with nuclear fast red.

2.6. Cell proliferation

The MTT reduction assay (Sigma–Aldrich, Taufkirchen, Germany) was performed according to the manufacturer's instructions. The cell number was calculated according to a standard curve and growth curves were prepared for three individual donors ($n = 3$).

2.7. Presentation of cell surface antigens

Fluorescent Activated Cell Sorting (FACS) analysis was performed to determine alterations in typically presented positive (CD44, CD73, CD105, and CD166) and negative (CD14, CD34, and CD45) surface antigens by MSCs after magnetic labeling. Antibodies were purchased and FACS analysis was performed as described previously with cells of three donors and data are given as mean percentage of positive cells ± standard deviation [28].

2.8. Multi-lineage differentiation

To determine detrimental effects of magnetic labeling on the tri-lineage differentiation capacity, SPION-labeled MSCs were cultivated under conditions that induce adipogenic, osteogenic and chondrogenic differentiation according to protocols described in previous studies [30,31]. Because chondrogenesis was impaired after MSC labeling with 25 μg Fe/ml Citrate SPIONs and 500 μg Fe/ml Endorem SPIONs, the effect of lower labeling concentrations (1 and 10 μg Fe/ml Citrate SPIONs, 10 and 100 μg Fe/ml Endorem SPIONs) was also investigated. Three sets of donor cells were subjected to differentiation for each lineage ($n = 3$).

2.9. Chemotaxis

The migration of (un)labeled MSCs towards 1000 nM CCL25 (TECK, thymus expressed chemokine; PeproTech, Hamburg, Germany) was investigated as described previously [28]. Dulbecco's modified Eagle's Medium (Biochrom, Berlin, Germany) supplemented with 0.1% FBS (Thermo Scientific Hyclone, Logan, USA) served as negative control and cultivation medium supplemented with 10% FBS was used as positive control. Because cell migration was significantly decreased for MSCs incubated with 25 μg Fe/ml Citrate SPIONs and 500 μg Fe/ml Endorem SPIONs, chemotactic potential of MSCs after labeling with lower concentrations of Citrate (5 and 10 μg Fe/ml) and Endorem (50 and 100 μg Fe/ml) SPIONs was also investigated. The assay was performed for three individual donors ($n = 3$) and data are shown as means ± standard deviation. To determine statistically ($P \leq 0.05$) altered migration of labeled MSCs compared to the respective unlabeled controls, one-way ANOVA followed by Bonferroni/Dunn post-hoc testing was applied.

2.10. Actin staining with fluorescent phallotoxins

Phalloidin is a toxin that selectively binds to F-actin and was used to visualize the organization of the cytoskeleton. Briefly, cells were fixed on chamber slides and permeabilized with 1% Triton X-100. Following incubation with phalloidin conjugated to fluorescent AlexaFluor 633 dye (Invitrogen, Darmstadt, Germany), the nuclei were stained by propidium iodide. Control and SPION-labeled cells were investigated using a confocal laser scanning microscope (CLSM; ZeissLSM 510 meta, Zeiss MicroImaging GmbH) equipped with 100× oil immersion objective, numerical aperture 1.3. Images of the samples were prepared in multi-track mode with separate excitation of propidium iodide and AlexaFluor 633 conjugated phalloidin (543 nm and 633 nm, respectively). The fluorescence was recorded in two channels with long-pass filters 560 nm for propidium iodide and 650 nm for phalloidin.

Different z-stacks of the samples were analyzed using the LSM 510 software and displayed as overlay modus of the two fluorescence channels in orthogonal section views.

2.11. MSC transplantation and in vivo MRI

Animal experiments were approved by the local legal representative (Landesamt für Gesundheit und Soziales, Berlin, Germany; Reg G0230/09) and were performed according to the institutional guidelines. Eight male Lewis rats weighing 250 g (Harlan-Winkelmann, Borchen, Germany) were anesthetized with 2–5% isoflurane (Forene, Abbot, Wiesbaden, Germany) in 0.2 l/min oxygen. Subsequently, 3.125×10^5 MSCs (25 μL) of a cell pool of 5 donors labeled with 5 μg Fe/ml Citrate SPIONs were injected into the left lower leg muscle and cells labeled with 100 μg Fe/ml Endorem SPIONs into the right lower leg muscle. During subsequent MRI examinations rats were anesthetized with isoflurane under constant ventilation monitoring (Small Animal Monitoring & Gating System, SA Instruments, Stony Brook, New York, USA). A heated circulating water blanket was used to ensure constant body temperature. The animals were placed on a custom-built animal holder with feet first and each lower leg was imaged individually. Imaging of the transplanted cells was carried out with T2*-weighted 2D-gradient-echo sequence (FLASH) with TR/TE = 892.4/5.4 ms, flip angle 40° and 4 averages. Axial and sagittal images with a slice thickness of 0.5 mm, a FOV of 45 × 45 mm and a matrix size of 256 × 256 were generated. MRI data processing was performed with Amira software (Version 4.1, Mercury Computer Systems, San Diego, USA). Hypointense areas of SPION-labeled MSCs were three-dimensionally reconstructed and volume and surface area of transplanted cells were calculated as means ± standard deviation ($n = 8$).

2.12. Ex vivo analysis

The muscle samples were fixated, dehydrated and embedded in paraffin. Prussian Blue staining was performed to retrieve SPION-labeled MSCs in the muscle tissue sections. Histological specimens containing iron-positive cells were subjected to hematoxylin and eosin (HE) staining and were stained immunohistochemically with monoclonal anti-CD44 (antibodies-online GmbH, Aachen, Germany) and anti-mitochondria MCT02 (Novus Biologicals, Littleton, USA) antibodies that selectively detect human MSCs in rat muscle tissue. Antibody staining was detected using the EnVision™ System Peroxidase (AEC) Mouse and Rabbit Kit (DAKO, Hamburg, Germany) according to the manufacturer's protocol.

3. Results

3.1. SPION characterization

The hydrodynamic diameters of all SPION types were comparable with values in the range between 80 and 160 nm as measured in distilled water (Resovist SPIONs, 84.44 ± 1.35 nm; Citrate SPIONs, 98.13 ± 1.23 nm and Endorem SPIONs, 157.33 ± 5.46 nm) (Table 1). At physiological ion concentration Resovist SPIONs are slightly negatively charged (−9.94 ± 1.45 mV), Endorem SPIONs are almost neutral (−3.48 ± 0.55 mV) and citrate-coated SPIONs possess a high negative surface charge (−27.3 ± 1.41 mV).

3.2. Dose- and type- dependent MSC labeling with SPIONs

The uptake of SPIONs by MSCs was dose- and type- dependent. The high efficacy of MSCs in internalizing Citrate SPIONs was clearly indicated by high intracellular iron concentrations measured by ICP-OES and visualized by intense Prussian Blue staining. The quantification of the iron uptake by human MSCs as function of the SPION Fe-concentration in the cultivation medium and of the SPION type is shown in Fig. 1A. Compared to the commercial nanoparticles, the Citrate SPIONs were effectively internalized by MSCs even at low SPION Fe-concentrations in the cultivation medium. At a Citrate SPION concentration of 25 μg Fe/ml in the cultivation medium, for example, the amount of internalized iron by MSCs reached 69.6 ± 5.1 pg Fe/cell. This intracellular iron content is remarkably higher than that obtained after incubation with Resovist (1.3 ± 2.3 pg Fe/cell) and Endorem (4.9 ± 2.7 pg Fe/cell) nanoparticles at the same SPION Fe-incubation concentration. Focusing on the SPION labeling concentrations that were comparatively investigated for all three SPION types (25, 50 and 100 μg Fe/ml), the internalization of Citrate SPIONs by human MSCs was more than one order of magnitude increased. This remarkably pronounced uptake of Citrate SPIONs by human MSCs compared to commercial SPIONs was also visualized by Prussian Blue staining (Fig. 1B). The blue staining of intracellular iron particles was most intense after incubation with Citrate SPIONs. Consistent with these results, human MSCs labeled with Citrate SPIONs gave rise to highest signal loss in the MRI (Fig. 1C, D). Labeled MSCs showed a trend of enhanced signal loss with increasing labeling concentration for all studied SPION types as shown in Fig. 1C (MR data as bar chart) and Fig. 1D (MR images of phantoms). Very importantly, MRI hypointensity was most intense for MSCs labeled with Citrate SPIONs compared to Resovist and Endorem particles at same SPION iron incubation concentrations in the cultivation medium.

3.3. Impact of magnetic labeling on MSC function

For investigating the cellular effects of magnetic labeling with experimental Citrate SPIONs, cells were incubated with 25 μg Fe/ml in the cultivation medium because this labeling concentration resulted in sufficient contrast in the MRI. Studies were also performed with one commercial SPION type, the Endorem nanoparticles, at a concentration of 500 μg Fe/ml because respective particle type and concentration are frequently described in literature and allow comparative investigations. All studies were performed in comparison to unlabeled cells. Incubation of MSCs with SPIONs resulted in approximately 100% of cells being labeled after counting Prussian Blue positive cells (data not shown). The intracellular iron content determined by ICP-OES amounted to 69.6 ± 5.1 pg (Citrate SPION) and 25.7 ± 6.5 pg (Endorem SPION). Adherent MSCs maintained the typical fibroblast-like morphology after magnetic labeling (Fig. 2A). Intracellular SPIONs were visualized in cell culture as brownish aggregates and as blue particles in Prussian Blue stains. Transmission electron microscopy visualized the internalized nanoparticles in intracellular endosomes. The growth curve of labeled MSCs was equivalent to unlabeled cells as shown in Fig. 2B for one representative donor. No significant cytotoxicity was observed. Furthermore, magnetic labeling did not alter the presentation of typical surface antigens on human MSCs. Almost 100% of labeled cells were positive for the typical MSC markers CD44, CD73, CD105 and CD166 and negative for CD14,

Table 1
Names and properties of investigated superparamagnetic iron oxide nanoparticles.

Name/company	Generic name	Particle size (nm)	Zeta potential (mV)	Iron oxide core size (nm)	Coating	Reference
		In aqua dest.	In 150 mM NaCl			
Resovist SPIONs/Bayer HealthCare	Ferucarbotran	84.44 ± 1.35	−9.94 ± 1.45	4.2	Carboxydextran	[11,18]
Endorem SPIONs/Guerbet	Ferumoxide	157.33 ± 5.46	−3.48 ± 0.55	4.2–4.8	Dextran	[11,53]
Citrate SPIONs/MagneticFluids	–	98.13 ± 1.23	−27.3 ± 1.41	6–7	Citrate	–

Particle sizes (hydrodynamic diameters) and zeta potentials were determined with the Zetasizer nano ZS and data are given as means ± SD. The iron oxide core size of citrate-coated SPIONs was determined by TEM. The size of the iron oxide cores and coating material of Resovist and Endorem SPIONs were taken from the literature. Abbreviations: aqua dest., distilled water; SPIONs, superparamagnetic iron oxide nanoparticles.

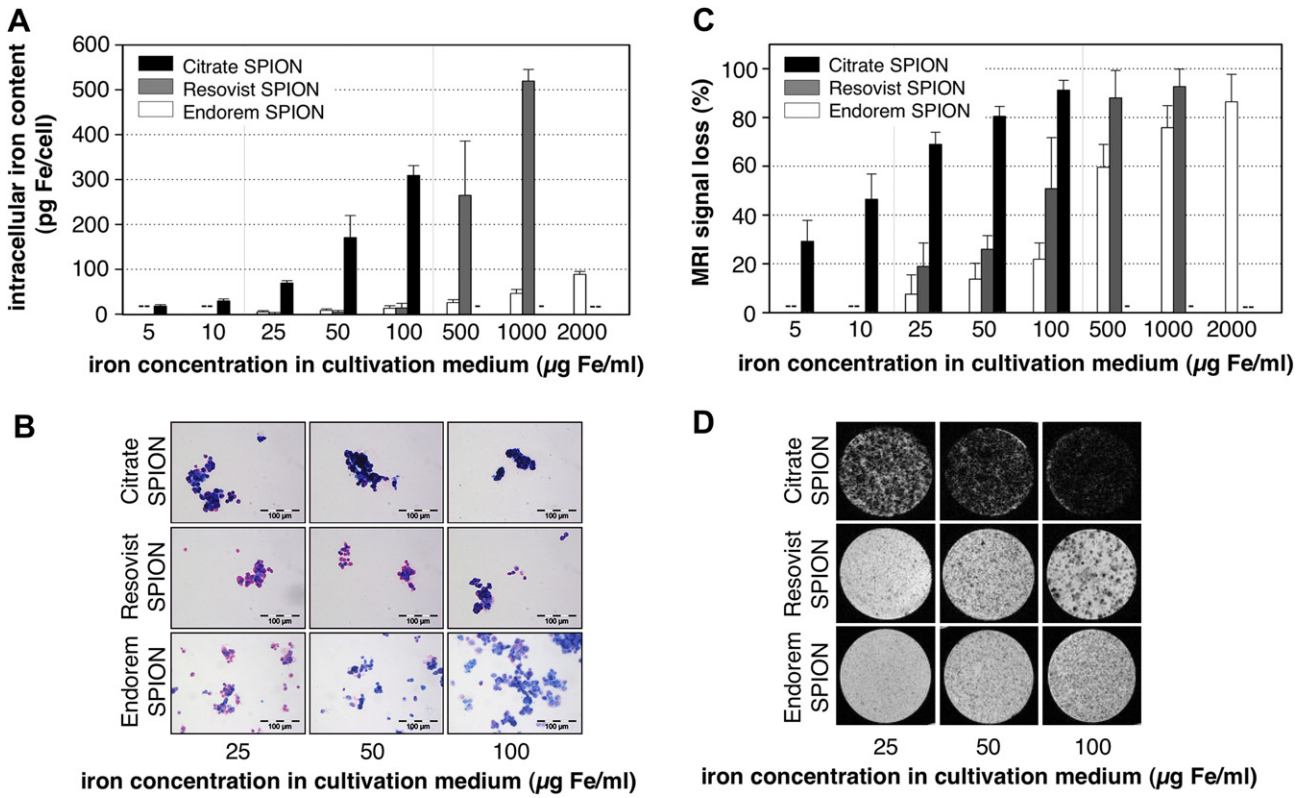

Fig. 1. Dose- and type- dependent MSC labeling with SPIONs. Adherent MSCs were incubated for 24 h with increasing concentrations of Citrate (5–100 μg Fe/ml), Resovist (25–1000 μg Fe/ml) and Endorem (25–2000 μg Fe/ml) SPIONs in the cultivation medium. Magnetic labeling of human MSCs was investigated as function of the SPION iron concentration in the cultivation medium and of the SPION type by quantification of the intracellular iron content using ICP-OES (A), Prussian Blue staining (B) and visualization by *in vitro* MRI (C and D). Internalization of Citrate SPIONs was more than one order of magnitude increased compared to the uptake of commercial Resovist and Endorem SPIONs as was clearly indicated by highest iron content per cell (A) and most intense Prussian Blue staining (B) at same iron labeling concentrations in the cultivation medium. Consistently, human MSCs labeled with Citrate SPIONs gave rise to highest signal loss in the MRI compared to commercial SPIONs (C, MR data as bar chart and D, MR images of phantoms). When indicated as "-", then not determined. Abbreviations: ICP-OES, inductively coupled plasma optical emission spectroscopy; MRI, magnetic resonance imaging; MSCs, mesenchymal stem cells; SPIONs, superparamagnetic iron oxide nanoparticles.

CD34 and CD45 (Table 2). In addition, both unlabeled and SPION-labeled cells showed a similar differentiation capacity into the adipogenic and osteogenic lineages (Fig. 3). Adipogenesis was demonstrated by the accumulation of lipid vacuoles indicated by a positive Oil Red O staining. Alkaline phosphatase and von Kossa staining confirmed osteogenic differentiation. In contrast, chondrogenesis was shown to be dependent from the intracellular SPION load (Fig. 3). Unlabeled MSCs and cells labeled with low SPION concentrations in the cultivation medium (1 μg Fe/ml Citrate SPIONs and ≤100 μg Fe/ml Endorem SPIONs) showed a considerable formation of proteoglycans as detected by Alcian Blue staining and showed positive collagen type II immunohistochemical stainings. In contrast, labeling with high SPION concentrations (≥10 μg Fe/ml Citrate SPIONs and 500 μg Fe/ml Endorem SPIONs) interfered with the formation of compact pellets and with the generation of proteoglycan- and collagen type II-positive extracellular matrix. Highly magnetically labeled MSCs failed to generate dense pellets and showed no evidence of chondrogenesis. All control stainings were negative for not-induced samples in any of the non-differentiation cultures (Fig. 3, small images at top left). Furthermore, a migration assay was performed to examine the effect of magnetic cell labeling on the chemotactic potential (Table 3). Migration of SPION-labeled MSCs was investigated towards a negative control (0.1% FBS), a positive control (10% FBS) and towards 1000 nM of the chemokine CCL25 and was compared to the migration of unlabeled cells. With increasing magnetic labeling, cell migration towards the chemokine and the positive control became significantly impaired. For the highest magnetic labeling concentrations examined (25 μg Fe/ml Citrate SPIONs and 500 μg Fe/ml Endorem SPIONs), migration of all three investigated donor cells towards the positive control was significantly decreased compared to the respective unlabeled control specimen.

3.4. *In vivo and ex vivo visualization of SPION-labeled MSCs*

A cellular transplantation experiment was conducted to test the sensitivity and efficacy of experimental Citrate SPIONs (5 μg Fe/ml) in comparison to commercial Endorem SPIONs (100 μg Fe/ml) as intracellular MSC labels for MRI. Transplanted cell numbers, volumes and SPION labeling concentrations were followed from results of preliminary *in vivo* experiments (data not shown). Subsequently after intramuscular injection of magnetically labeled MSCs, areas of transplanted cells of both SPION labeling types appeared clearly hypointense in rat muscle tissue in MR images (Fig. 4A, white arrowheads). Although labeled with the 20-fold SPION iron concentration, transplanted Endorem-MSCs showed a considerable smaller volume (11.4 ± 1.2 mm^3) and surface area (14.6 ± 5 mm^2) of hypointensity than cells that have been labeled with Citrate SPIONs (volume 23.4 ± 2 mm^3, surface area 46.6 ± 4.6 mm^2) (Fig. 4B). However, both SPION types can be used to detect labeled MSCs by MRI after transplantation, albeit a considerable lower labeling concentration is required for Citrate SPIONs than for Endorem SPIONs.

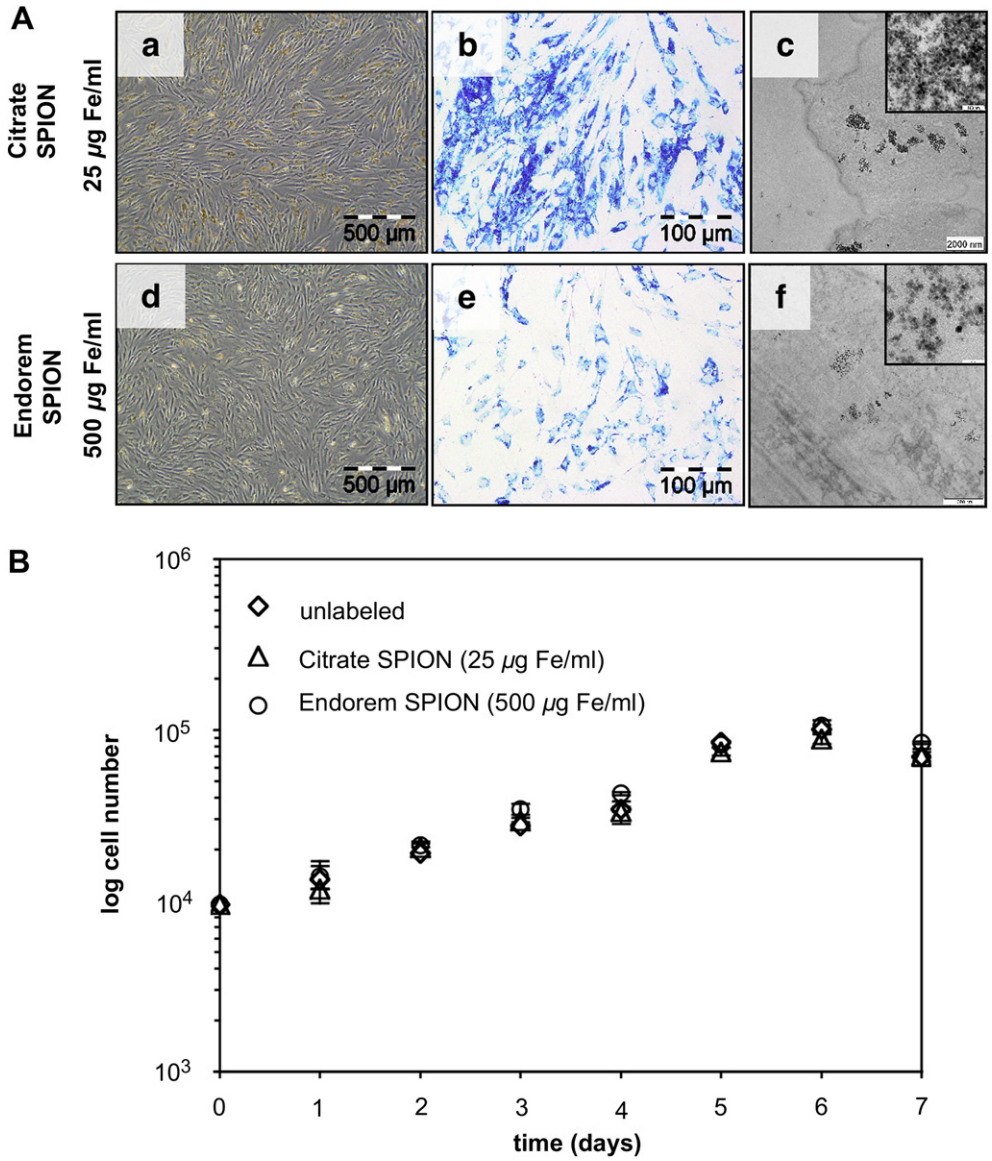

Fig. 2. Visualization of intracellular SPIONs (A) and proliferation assay (B). After incubation of human MSCs with Citrate (25 µg Fe/ml, a–c) and Endorem (500 µg Fe/ml, d–f) SPIONs internalized iron oxide nanoparticles were visualized during cell culture, by Prussian Blue staining and by transmission electron microscopy. The proliferation of human MSCs was not affected by magnetic labeling with Citrate and Endorem SPIONs as determined by MTT reduction assay (B). The growth curves of labeled MSCs and unlabeled controls exhibit almost the same shape as shown here exemplarily for one representative donor. Abbreviation: SPIONs, superparamagnetic iron oxide nanoparticles.

Histological analyses of animals were performed directly after transplantation and MR imaging to correlate the MRI findings with immunostaining evidence of cell and label fate (Fig. 4C). For both SPION labeling types, Prussian Blue positive cells were retrieved in the muscle tissue and respective cells showed positive immunohistochemical staining with human-specific anti-mitochondrial MCT02 and MSC-specific anti-CD44 antibodies. Both antibodies did not stain rat muscle cells.

4. Discussion

Magnetic resonance imaging is an attractive tool to *in vivo* monitor transplanted cells with high spatiotemporal, repeated and non-invasive visualization. The sensitive MRI detection of magnetically labeled MSCs requires the sufficient intracellular uptake of MR contrast agents. Superparamagnetic iron oxide nanoparticles are preferred to gadolinium chelates for cell labeling because they provide high signal contrasts in T2/T2*-weighted image sequences, are nontoxic and biodegradable and can be coated with functional ligands for a more efficient and/or specific internalization. Among the different SPIONs that are commercialized for clinical use, Endorem and Resovist are most accomplished. Though these commercial SPIONs are highly phagocyted by Kupffer cells and are therefore clinically used to achieve liver and spleen imaging, they do not allow efficient cellular uptake by MSCs as these cells lack substantial phagocytic capacity. So far, different strategies have been described to further enhance the uptake of these commercial SPIONs by MSCs. The primary approach involves the use of transfection agents that facilitate the non-specific SPION uptake by providing high affinity to the cellular membrane [20,32]. The group of Bulte was the first that directly linked transfection agents to SPIONs, so-called magnetodendrimers, to efficiently magnetically label MSCs [33]. However, the ratio of transfection agent and SPIONs needs to be carefully titrated to provide a stable

Table 2
Cell surface marker analysis of unlabeled and SPION-labeled (25 μg Fe/ml Citrate SPIONs, 500 μg Fe/ml Endorem SPIONs) human MSCs.

CD markers	Unlabeled MSCs	MSCs labeled with Citrate SPIONs	MSC labeled with Endorem SPIONs
CD14	0.2% ± 0.2%	0.1% ± 0.1%	0.1% ± 0.0%
CD34	0.1% ± 0.1%	0.2% ± 0.2%	0.0% ± 0.0%
CD45	0.1% ± 0.1%	0.1% ± 0.2%	0.0% ± 0.0%
CD44	98.6% ± 2.0%	99.1% ± 0.7%	99.9% ± 0.1%
CD73	99.9% ± 0.0%	99.3% ± 0.5%	100.0% ± 0.0%
CD105	99.1% ± 0.6%	98.6% ± 0.8%	99.2% ± 1.0%
CD166	99.1% ± 1.2%	98.3% ± 0.8%	99.8% ± 0.1%

Typical negative (CD14, CD34 and CD45) and positive (CD44, CD73, CD105 and CD166) cell surface markers of human MSCs are shown as means ± SD. Abbreviations: CD, cluster of differentiation; MSCs, mesenchymal stem cells; SPIONs, superparamagnetic iron oxide nanoparticles.

complex because insufficiently complexed transfection agents are cytotoxic [34]. Another approach for an efficient magnetic labeling is to link translocating peptides to the SPION surface, such as HIV Tat, that also facilitates particle internalization [35,36]. However, the HIV tat peptide fosters the SPION accumulation in the nucleus and thus, may potentially interfere with nucleus function [20]. Last but not least, another approach is to covalently link the magnetic particles with high affinity ligands such as antigen-specific monoclonal antibodies that specifically bind to a distinct cell type and enter the cell through receptor-mediated endocytosis [37–39]. Though this strategy offers a specific SPION uptake, it requires the availability of an internalized monoclonal antibody and furthermore, the number of cell membrane receptors is limiting the internalization efficiency. Thus, strategies to yield an efficient internalization of commercial SPIONs by MSCs entail potential disadvantages in terms of technically complex surface modifications, poor availability and biocompatibility/biosafety issues. Therefore, the development of a non-derivatized SPION type that can be efficiently internalized by MSCs without requiring transfection agents for *in vivo* tracking by MRI is of great interest.

Because it is well established that size and surface properties affect the SPION internalization, magnetic MSC labeling with new experimental anionic SPIONs was investigated in comparison to commercial SPIONs of comparable size but of different surface charges. As summarized in Table 1, dextran-coated Endorem SPIONs are almost neutral at physiological ion concentrations. Resovist SPIO nanoparticles are coated with carboxydextran that

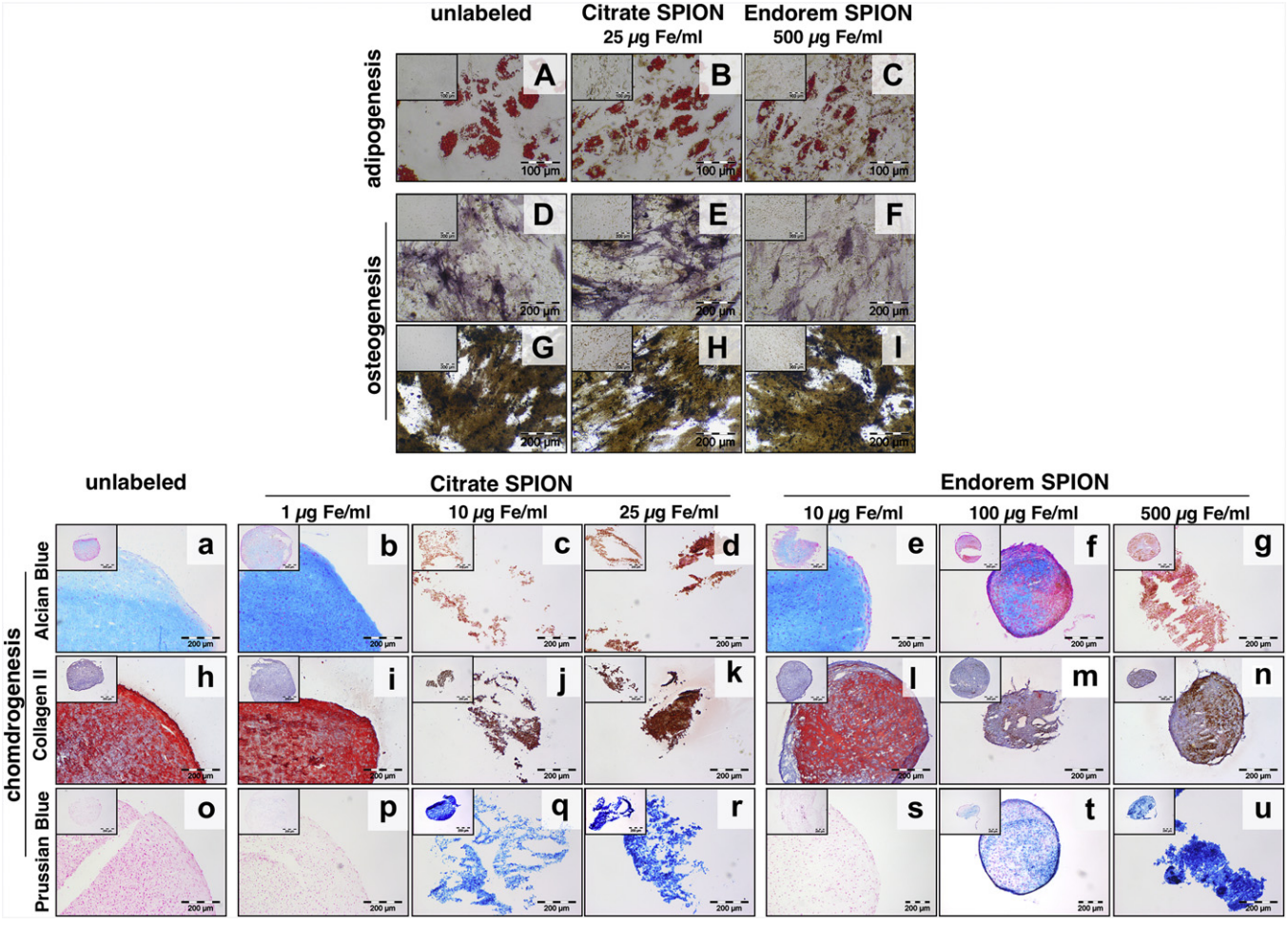

Fig. 3. Multi-lineage differentiation capacity of SPION-labeled MSCs. Magnetically labeled and unlabeled MSCs were differentiated into the adipogenic, osteogenic and chondrogenic lineages. Adipogenic and osteogenic differentiation were not affected after labeling cells with 25 μg Fe/ml Citrate SPIONs (B, E, H) and 500 μg Fe/ml Endorem SPIONs (C, F, I). Lipid accumulation was observed as a result of adipogenic induction in unlabeled (A) and SPION-labeled (B, C) MSCs. Alkaline Phosphatase activity was increased compared to not-induced controls (D–F) and von Kossa stained cultures showed large calcium nodules (G–I) for both labeled and unlabeled cells. In contrast, human MSCs labeled with ≥10 μg Fe/ml Citrate SPIONs and 500 μg Fe/ml Endorem SPIONs failed to generate compact pellets and did not synthesize Alcian Blue- (c, d, g) and collagen type II- (j, k, n) positive extracellular matrix as were synthesized by unlabeled (a, h) and low magnetically labeled cells (1 μg Fe/ml Citrate SPIONs (b, i) and 10 (e, l) and 100 (f, m) μg Fe/ml Endorem SPIONs) after 28 days of micromass culture. Prussian Blue staining (o–u) revealed iron-positive cells within the micromass cultures of labeled cells (≥10 μg Fe/ml Citrate SPIONs (q, r) and ≥100 μg Fe/ml Endorem SPIONs (t, u)). As controls, all stainings were negative for not-induced samples in any of the non-differentiation cultures (small images at top left). Abbreviation: SPIONs, superparamagnetic iron oxide nanoparticles. (For interpretation of the references to colour in this figure legend, the reader is referred to the web version of this article.)

Table 3
Number of cells migrating towards the chemokine CCL25 at 1000 nM and respective negative and positive controls. Human MSCs were labeled with Citrate SPIONs (5 μg Fe/ml, 10 μg Fe/ml, 25 μg Fe/ml) and Endorem SPIONs (50 μg Fe/ml, 100 μg Fe/ml, 500 μg Fe/ml), respectively. Unlabeled cells were used as controls. The intracellular iron content was determined with ICP-OES.

Citrate SPION					
Iron concentration in cultivation medium (μg Fe/ml)		Unlabeled	5	10	25
Intracellular iron content (pg Fe/cell)		0.75 ± 0.7	18.3 ± 3.0	29.6 ± 4.1	69.6 ± 5.1
Donor 1	Neg	914.8 ± 161.7	1027.8 ± 131.5	408.9 ± 177.8	801.8 ± 82.8
	CCL25	3449.2 ± 150.0	**2233.1 ± 482.2*** ($P = 0.002$)	**1770.3 ± 178.5*** ($P < 0.001$)	**1076.2 ± 91.8*** ($P < 0.001$)
	Pos	10,433.6 ± 394.2	10,718.8 ± 630.4	**7651.6 ± 206.1***($P < 0.001$)	**6473.2 ± 147.9*** ($P < 0.001$)
Donor 2	Neg	86.1 ± 94.6	220.6 ± 129.5	258.3 ± 42.7	75.3 ± 51.9
	CCL25	2545.2 ± 276.9	**1092.3 ± 276.9*** ($P < 0.001$)	**1485.1 ± 58.2*** ($P < 0.001$)	**796.4 ± 131.5*** ($P < 0.001$)
	Pos	5698.4 ± 444.1	5773.7 ± 631.9	**4509.2 ± 404.0*** ($P = 0.034$)	**3750.5 ± 181.4*** ($P = 0.002$)
Donor 3	Neg	511.2 ± 79.6	414.3 ± 72.8	570.4 ± 144.7	**107.6 ± 24.7*** ($P = 0.002$)
	CCL25	2808.8 ± 375.5	2631.3 ± 113.0	2663.5 ± 397.7	**1103.1 ± 105.0*** ($P < 0.001$)
	Pos	4277.8 ± 422.2	3766.6 ± 121.2	**3320.0 ± 220.3*** ($P = 0.008$)	**2346.1 ± 233.5*** ($P < 0.001$)

Endorem SPION					
Iron concentration in cultivation medium (μg Fe/ml)		Unlabeled	50	100	500
Intracellular iron content (pg Fe/cell)		2.8 ± 2.1	8.4 ± 3.2	13.2 ± 5.5	25.7 ± 6.5
Donor 4	Neg	742.6 ± 299.0	769.4 ± 162.5	306.7 ± 80.7	**285.2 ± 119.0*** ($P = 0.049$)
	CCL25	3153.2 ± 299.5	2593.6 ± 429.0	2636.6 ± 233.0	**1463.6 ± 426.3*** ($P = 0.001$)
	Pos	10,444.3 ± 784.0	10,132.2 ± 297.8	8770.9 ± 33.6	**8001.4 ± 242.3*** ($P < 0.05$)
Donor 5	Neg	887.8 ± 241.1	1065.4 ± 213.5	780.2 ± 188.5	785.6 ± 72.8
	CCL25	2211.6 ± 55.9	2001.7 ± 227.7	2491.4 ± 245.0	**1043.9 ± 203.1*** ($P < 0.001$)
	Pos	7221.2 ± 510.8	7743.1 ± 578.7	7979.9 ± 579.6	**5499.3 ± 442.8*** ($P = 0.012$)
Donor 6	Neg	791.0 ± 105.8	898.6 ± 261.0	640.3 ± 121.2	801.8 ± 67.2
	CCL25	1673.5 ± 296.0	1560.5 ± 163.3	1512.0 ± 137.3	1178.4 ± 70.4
	Pos	8518.0 ± 848.4	8808.5 ± 621.9	8243.5 ± 417.9	**6521.7 ± 121.9*** ($P = 0.008$)

Data are shown as means ± SD. *Migration is significantly decreased compared to the respective unlabeled specimen, one-way ANOVA followed by Bonferroni/Dunn post-hoc testing, $P \leq 0.05$. Abbreviations: ICP-OES, inductively coupled plasma optical emission spectroscopy; MSCs, mesenchymal stem cells; SPIONs, superparamagnetic iron oxide nanoparticles.
Bold values represent the *P*-values for significant cell migration numbers

gives a slight net negative charge. The experimental SPIONs are highly negatively charged due to stabilization of the iron cores with citrate. When comparing both commercial SPIONs, the cellular uptake of Resovist was elevated at higher labeling concentrations compared to Endorem. This is in line with data recently published by Mailänder and colleagues [40]. This group also reported that with increasing the density of carboxyl groups on the particle surface, the Resovist SPION uptake was even further enhanced indicating strongly the relevance of the negative surface charge on particle internalization. Consistently, when employing the same SPION Fe-concentration in the cultivation medium, internalization of the highly negatively charged experimental Citrate SPIONs was remarkably increased compared to the commercial SPIONs as shown by highest intracellular iron uptake, highest MRI contrast and most intense Prussian Blue staining. To achieve equivalent loading of MSCs, commercial SPIONs have to be employed with an about 20-fold higher concentration in the cultivation medium compared to Citrate SPIONs. In line with these findings, Fleige and co-workers showed that internalization of citrate-coated ultrasmall SPIONs by macrophages is considerably elevated compared to the uptake of carboxydextran-coated ultrasmall nanoparticles [27]. As shown by TEM images, incubation of human MSCs with Citrate SPIONs resulted in the internalization into endosomes suggesting an endocytotic uptake mechanism as already described for the investigated commercial nanoparticles [18,41]. Wilhelm and colleagues attributed the highly efficient uptake of anionic SPIONs to internalization through a non-specific adsorptive endocytotic pathway [23,24]. Briefly, highly negatively charged SPIONs repulsively interact with negative domains of the plasma membrane, induce local neutralization and unspecifically adsorb on the cell membrane with subsequent membrane bending and efficient capturing into endosomal compartments. Safi and colleagues assumed furthermore that highly efficient internalization of SPIONs coated with anionic monomers is due to their destabilization in physiological culture medium [26]. Consistently, the size of the investigated commercial SPIONs remained constant, whereas the hydrodynamic diameter of citrate-coated SPIONs considerably increased at physiological ion concentration (Fig. 5A). In agreement with results from Safi et al. we hypothesize that the initially fine dispersed Citrate SPIONs destabilize in cultivation medium, aggregate and settle down to the bottom of the cell culture flask where they accumulate at the cell membranes that effectively promotes internalization. Aggregated Citrate SPIONs increased more than one order of magnitude in size suggesting also a size-dependent uptake effect as already reported by others for different nanoparticles and mammalian cells [41–43]. Thus, highly efficient magnetic labeling of human MSCs with Citrate SPIONs may be explained by an altered endocytotic uptake mechanism due to the highly negative surface charge and/or due to increase in size after aggregation in cultivation medium.

A mandatory prerequisite for a magnetic cell labeling technique is to preserve the normal cell function. Until now, there are no published data on the impact of highly anionic SPION uptake on the properties of human stem cells. In this study, no detrimental effects of magnetic labeling on the presentation of cell surface phenotypic markers, cell proliferation and differentiation into the adipogenic and osteogenic lineages were observed.

However, migration towards the chemokine CCL25 and chondrogenic differentiation were impaired dose-dependently with the SPION load. Irrespective of the SPION type used for magnetic cell labeling, previous studies did hardly examine the impact on chemotaxis. Solely the group of Schäfer reported recently in line with our findings that MSC migration towards a chemoattractant (PDGF-BB) was significantly reduced after magnetic labeling [44].

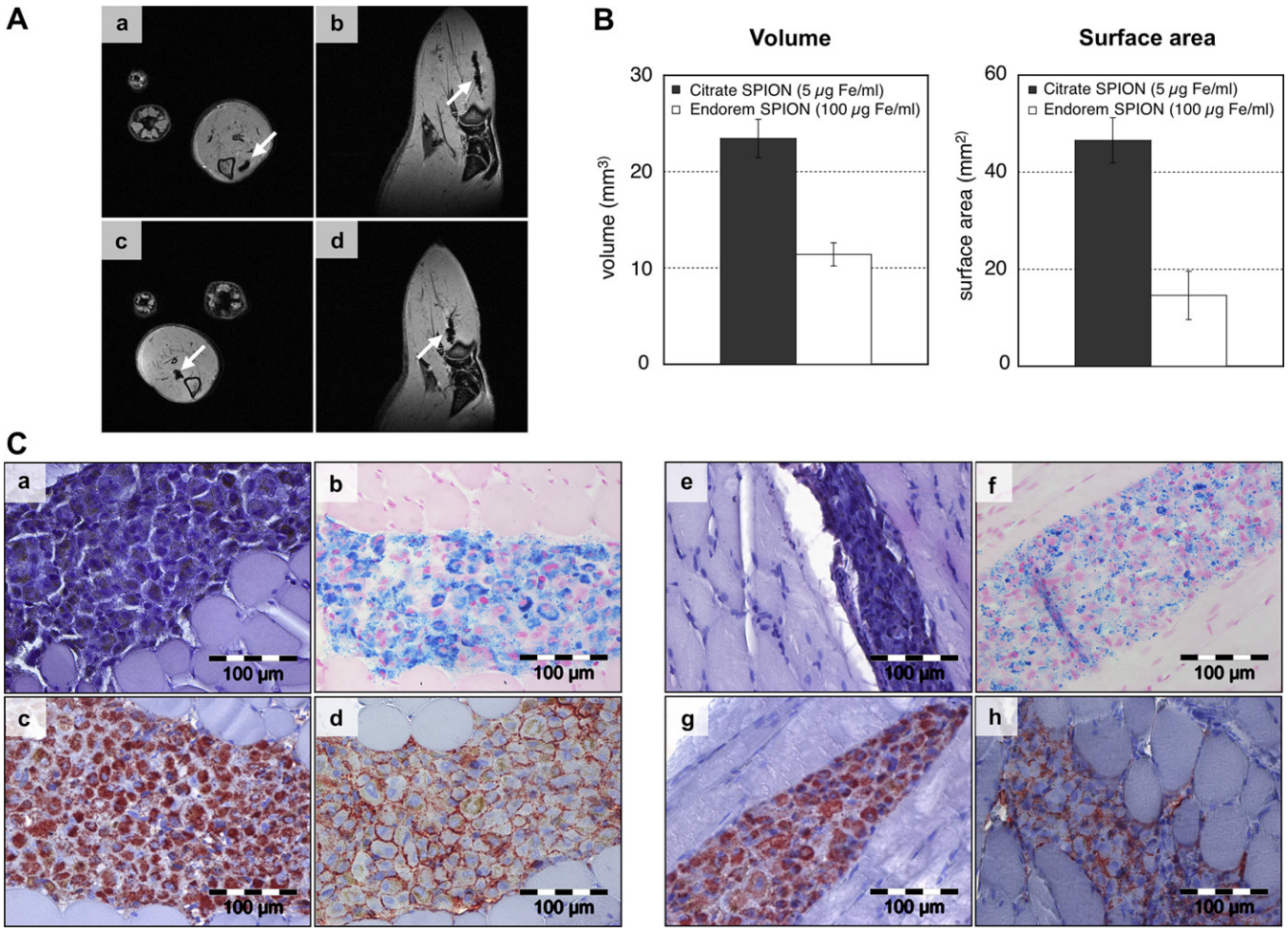

Fig. 4. *In vivo* and *ex vivo* visualization of SPION-labeled MSCs. *In vivo* MR imaging showed areas of hypointensity in rat muscle tissue in the axial (A; a, c) and sagittal (A; b, d) view albeit with a larger area of hypointensity seen for Citrate SPION-labeled MSCs (A; a, b) than for Endorem SPION-labeled cells (A; c, d). Consistently, transplanted Citrate SPION-labeled MSCs showed considerably higher hypointense volume and surface area compared to Endorem SPION-labeled cells (B). Hematoxylin and Eosin (C; a, e) and Prussian Blue (C; b, f) staining of muscle samples with transplanted Citrate (C, left) and Endorem (C, right) SPION-labeled MSCs demonstrated iron-loaded cells at the injection site. Immunohistochemical stainings of adjacent sections showed these cells to be human MSCs as detected positive for human-specific mitochondrial MCT02 (C; c, g) and for MSC-specific CD44 (C; d, h). Abbreviation: MRI, magnetic resonance imaging; MSCs, mesenchymal stem cells; SPIONs, superparamagnetic iron oxide nanoparticles.

We chose the chemokine CCL25 because it is a potent chemoattractant for MSCs as has previously been reported by Binger et al. [28].

Until now, the impact of SPION labeling on the chondrogenesis of human MSCs is an issue of debate. Earlier reports by the group of Bulte determined an impaired chondrogenic differentiation of SPION-labeled MSCs and they assumed the intracellular SPIONs to interfere with signaling processes required for mesenchymal condensation or to dysregulate the iron metabolism potentially involved in chondrogenesis [45,46]. Henning et al. reported that magnetic labeling of human MSCs with Resovist SPIONs inhibits chondrogenesis in a dose-dependent manner [47]. In contrast, numerous other groups showed that magnetic labeling does not affect chondrogenic differentiation of MSCs [44,48–50]. Confirming the findings published by Henning et al. this study revealed a dose-dependent impairment of the magnetic labeling concentration on chondrogenesis for both experimental citrate-coated and commercial dextran-coated SPIONs suggesting that the cause lies not with the type of particle or transfection agent but with the intracellular SPION load. High intracellular SPION concentrations have been shown to interfere with the organization of the cytoskeleton [51]. Thus, we performed actin staining of human MSCs that have been loaded with Citrate and Endorem SPIONs, respectively, at labeling concentrations that considerably impaired chondrogenesis and cell migration. The F-actin appeared organized as well-defined, clearly visible and single fibers in unlabeled cells. In contrast, disorganization of the actin network was observed within the cell where iron particles were located as illustrated by black intracellular spots (Fig. 5B). Furthermore, diminished cell spreading and clear areas of actin spotting indicating actin polymerization were observed in SPION-labeled MSCs. Since high SPION loading concentrations seem to interfere with the organization of the actin network this may cause detrimental effects on cell functions that involve remodeling of the cytoskeleton, such as chondrogenesis (mesenchymal condensation) and cell migration and thus, inhibit these processes dose-dependently. Consistently, a recently published study by Nohroudi et al. reported that the migratory potential of MSCs is negatively correlated with the SPION load and they also suggested a disturbed organization of the cytoskeleton as possible explanation [52]. Since chondrogenesis and migration were affected with increasing SPION load, a careful titration of the SPION labeling dose and MRI sensitivity is required to ensure full stem cell properties essential for cell-based therapeutic applications.

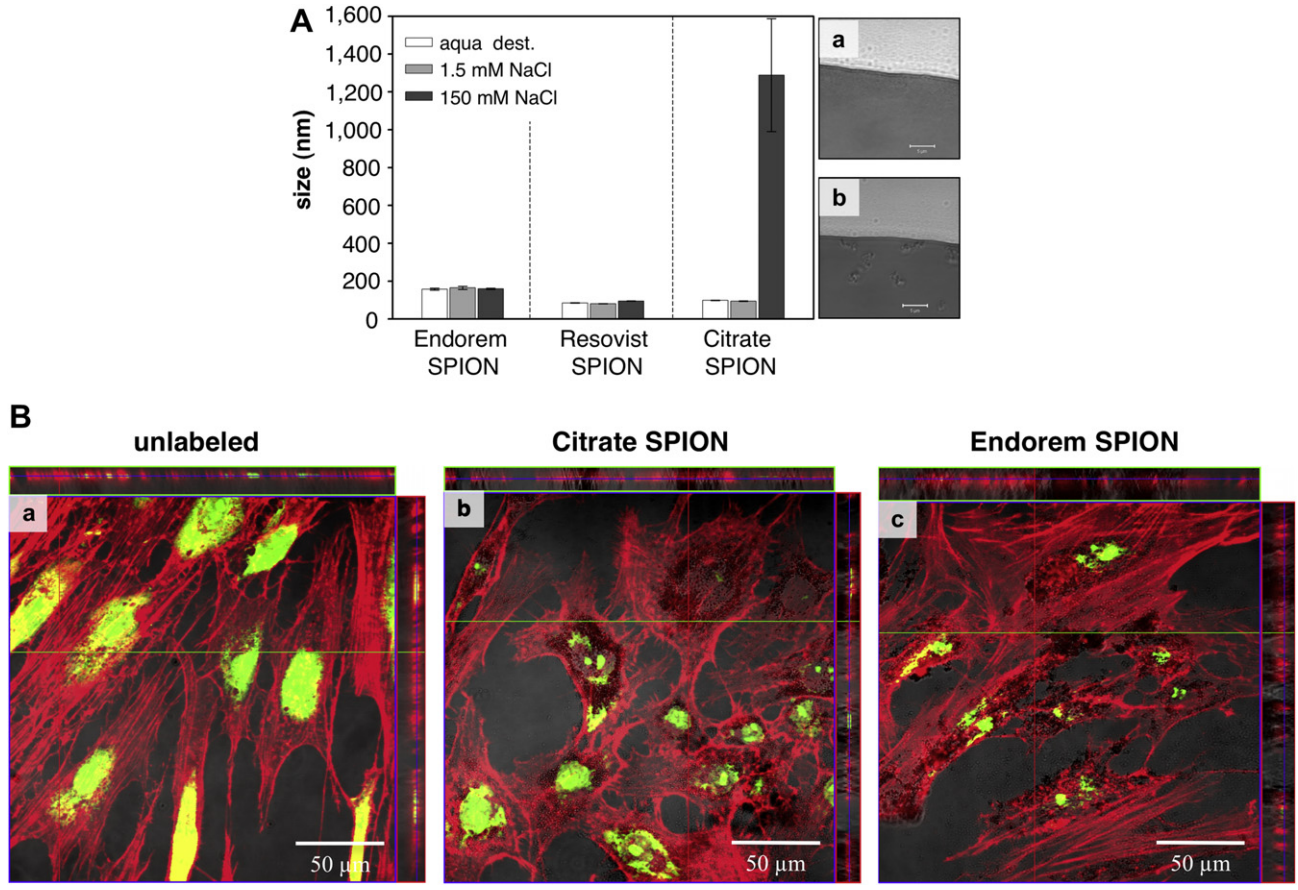

Fig. 5. Aggregation of Citrate SPIONs in cultivation medium (A) and disturbance of actin organization after SPION loading of MSCs (B). The hydrodynamic diameter of Endorem and Resovist SPIONs remained constant in distilled water, 1.5 mM and 150 mM sodium chloride. In contrast, size of Citrate SPIONs increased more than one order of magnitude at physiological ion concentrations (A). While commercial SPIONs remained homogeneously distributed in cultivation medium (A; a), particle aggregation was observed for Citrate SPIONs by confocal laser scanning microscopy (A; b). High intracellular SPION concentrations affect organization of the cytoskeleton of human MSCs (B) as shown by confocal micrographs in orthogonal section view of untreated MSCs (B; a), labeled with 25 µg/ml Citrate SPIONs (B; b) or 500 µg/ml Endorem SPIONs (B; c). F-Actin was stained with fluorescent phalloidin (red) and the nucleus with propidium iodide (green). Whereas F-actin fibers of unlabeled MSCs appeared highly organized, SPION-loaded cells exhibit disturbed organization of the cytoskeleton where black iron oxide nanoparticles were visible intracellularly. Abbreviation: SPIONs, superparamagnetic iron oxide nanoparticles. (For interpretation of the references to colour in this figure legend, the reader is referred to the web version of this article.)

In keeping with the efficient magnetic labeling of human MSCs with Citrate SPIONs over Endorem nanoparticles, the *in vivo* hypointensities developing in the muscle appeared more striking in rats transplanted with Citrate- than Endorem-MSCs although labeled with the twentieth SPION Fe-concentration in the cultivation medium. After image-based quantitative cellular detection, transplanted Citrate SPION-labeled cells showed higher volume and surface area than animals that have been transplanted with Endorem-labeled cells providing a considerably higher sensitivity for cellular detection. Immunohistochemical analysis of the harvested muscle tissues determined transplanted cells that were positive for iron by Prussian Blue stain and that were also positive for the human-specific markers anti-mitochondria and anti-CD44. Thus, new experimental Citrate SPIONs are attractive intracellular magnetic labels for MSCs to be visualized after transplantation *in vivo* by MRI and to be retrieved and confirmed *ex vivo* by Prussian Blue and specific immunohistochemical stainings.

5. Conclusions

In this study, highly efficient MSC labeling with new anionic citrate-coated SPIONs without requiring transfection agents was reported. Greater MRI sensitivity for visualization of transplanted cells labeled with Citrate SPIONs than with commercial SPIONs was demonstrated enabling better MRI *in vivo* tracking of transplanted cells. Hence, Citrate SPIONs are attractive candidates as efficient intracellular magnetic labels for MSCs. Since chondrogenic differentiation and chemotaxis were affected dose-dependently, a careful titration and optimization of SPION labeling doses are critical issues to be addressed in order to maintain full stem cell properties. However, efficient intracellular loading of low Citrate SPION concentrations can yield both sufficient contrast in the MRI and maintenance of cell viability and function important for cell-based therapies.

Conflict of interest

The authors confirm that there are no known conflicts of interest associated with this publication.

Acknowledgments

The Citrate SPIONs were kindly provided by Norbert Buske (MagneticFluids, www.magneticfluids.de). The authors are grateful to Harald Link (Institute of Materials Science and Technologies, Technical University Berlin, Germany) for the iron quantification with ICP-OES and to Rona Pitschke (Max Planck Institute of Colloids and Interfaces, Golm, Germany) for performing TEM imaging. We

thank Anja Wachtel and Johanna Golla for excellent technical assistance. We are very grateful to Kirsten Führer for her help in conducting the animal experiments. Furthermore, the authors gratefully acknowledge the experimental work of Karolina Grzeschik, Luise Bernhardt, Matthias Friedrich, Sabrina Prodlik and Anne Müller during their apprenticeships. This study was supported by the Bundesministerium für Bildung und Forschung (Grant: BMBF 0313911) and by the Deutsche Forschungsgemeinschaft (Grant: DFG SI 569/7-1).

References

[1] Ceradini DJ, Kulkarni AR, Callaghan MJ, Tepper OM, Bastidas N, Kleinman ME, et al. Progenitor cell trafficking is regulated by hypoxic gradients through HIF-1 induction of SDF-1. Nat Med 2004;10(8):858–64.
[2] Barry FP, Murphy JM. Mesenchymal stem cells: clinical applications and biological characterization. Int J Biochem Cell Biol 2004;36(4):568–84.
[3] Wang Y, Deng Y, Zhou GQ. SDF-1alpha/CXCR4-mediated migration of systemically transplanted bone marrow stromal cells towards ischemic brain lesion in a rat model. Brain Res 2008;1195:104–12.
[4] Chamberlain G, Fox J, Ashton B, Middleton J. Concise review: mesenchymal stem cells: their phenotype, differentiation capacity, immunological features, and potential for homing. Stem Cells 2007;25(11):2739–49.
[5] Honmou O, Houkin K, Matsunaga T, Niitsu Y, Ishiai S, Onodera R, et al. Intravenous administration of auto serum-expanded autologous mesenchymal stem cells in stroke. Brain 2011;134(Pt 6):1790–807.
[6] Assis AC, Carvalho JL, Jacoby BA, Ferreira RL, Castanheira P, Diniz SO, et al. Time-dependent migration of systemically delivered bone marrow mesenchymal stem cells to the infarcted heart. Cell Transplant 2010; 19(2):219–30.
[7] Krause U, Harter C, Seckinger A, Wolf D, Reinhard A, Bea F, et al. Intravenous delivery of autologous mesenchymal stem cells limits infarct size and improves left ventricular function in the infarcted porcine heart. Stem Cells Dev 2007;16(1):31–7.
[8] Granero-Molto F, Weis JA, Miga MI, Landis B, Myers TJ, O'Rear L, et al. Regenerative effects of transplanted mesenchymal stem cells in fracture healing. Stem Cells 2009;27(8):1887–98.
[9] Bulte JW, Duncan ID, Frank JA. In vivo magnetic resonance tracking of magnetically labeled cells after transplantation. J Cereb Blood Flow Metab 2002;22(8):899–907.
[10] Bulte JW. In vivo MRI cell tracking: clinical studies. AJR Am J Roentgenol 2009; 193(2):314–25.
[11] Wang YX, Hussain SM, Krestin GP. Superparamagnetic iron oxide contrast agents: physicochemical characteristics and applications in MR imaging. Eur Radiol 2001;11(11):2319–31.
[12] Bernsen MR, Moelker AD, Wielopolski PA, van Tiel ST, Krestin GP. Labelling of mammalian cells for visualisation by MRI. Eur Radiol 2010;20(2):255–74.
[13] Bos C, Delmas Y, Desmouliere A, Solanilla A, Hauger O, Grosset C, et al. In vivo MR imaging of intravascularly injected magnetically labeled mesenchymal stem cells in rat kidney and liver. Radiology 2004;233(3):781–9.
[14] Ju S, Teng GJ, Lu H, Jin J, Zhang Y, Zhang A, et al. In vivo differentiation of magnetically labeled mesenchymal stem cells into hepatocytes for cell therapy to repair damaged liver. Invest Radiol 2010;45(10):625–33.
[15] Kim YJ, Huh YM, Choe KO, Choi BW, Choi EJ, Jang Y, et al. In vivo magnetic resonance imaging of injected mesenchymal stem cells in rat myocardial infarction; simultaneous cell tracking and left ventricular function measurement. Int J Cardiovasc Imaging 2009;25(Suppl. 1):99–109.
[16] Winkler T, von Roth P, Schuman MR, Sieland K, Stoltenburg-Didinger G, Taupitz M, et al. In vivo visualization of locally transplanted mesenchymal stem cells in the severely injured muscle in rats. Tissue Eng Part A 2008;14(7): 1149–60.
[17] Jendelova P, Herynek V, Urdzikova L, Glogarova K, Kroupova J, Andersson B, et al. Magnetic resonance tracking of transplanted bone marrow and embryonic stem cells labeled by iron oxide nanoparticles in rat brain and spinal cord. J Neurosci Res 2004;76(2):232–43.
[18] Reimer P, Balzer T. Ferucarbotran (Resovist): a new clinically approved RES-specific contrast agent for contrast-enhanced MRI of the liver: properties, clinical development, and applications. Eur Radiol 2003;13(6):1266–76.
[19] Babic M, Horak D, Trchova M, Jendelova P, Glogarova K, Lesny P, et al. Poly(L-lysine)-modified iron oxide nanoparticles for stem cell labeling. Bioconjug Chem 2008;19(3):740–50.
[20] Frank JA, Miller BR, Arbab AS, Zywicke HA, Jordan EK, Lewis BK, et al. Clinically applicable labeling of mammalian and stem cells by combining superparamagnetic iron oxides and transfection agents. Radiology 2003;228(2): 480–7.
[21] Mahmoudi M, Hosseinkhani H, Hosseinkhani M, Boutry S, Simchi A, Journeay WS, et al. Magnetic resonance imaging tracking of stem cells in vivo using iron oxide nanoparticles as a tool for the advancement of clinical regenerative medicine. Chem Rev 2011;111(2):253–80.
[22] Frank JA, Zywicke H, Jordan EK, Mitchell J, Lewis BK, Miller B, et al. Magnetic intracellular labeling of mammalian cells by combining (FDA-approved) superparamagnetic iron oxide MR contrast agents and commonly used transfection agents. Acad Radiol 2002;9(Suppl. 2):S484–7.
[23] Wilhelm C, Billotey C, Roger J, Pons JN, Bacri JC, Gazeau F. Intracellular uptake of anionic superparamagnetic nanoparticles as a function of their surface coating. Biomaterials 2003;24(6):1001–11.
[24] Wilhelm C, Gazeau F. Universal cell labelling with anionic magnetic nanoparticles. Biomaterials 2008;29(22):3161–74.
[25] Billotey C, Wilhelm C, Devaud M, Bacri JC, Bittoun J, Gazeau F. Cell internalization of anionic maghemite nanoparticles: quantitative effect on magnetic resonance imaging. Magn Reson Med 2003;49(4):646–54.
[26] Safi M, Sarrouj H, Sandre O, Mignet N, Berret JF. Interactions between sub-10-nm iron and cerium oxide nanoparticles and 3T3 fibroblasts: the role of the coating and aggregation state. Nanotechnology 2010;21(14):145103.
[27] Fleige G, Seeberger F, Laux D, Kresse M, Taupitz M, Pilgrimm H, et al. In vitro characterization of two different ultrasmall iron oxide particles for magnetic resonance cell tracking. Invest Radiol 2002;37(9):482–8.
[28] Binger T, Stich S, Andreas K, Kaps C, Sezer O, Notter M, et al. Migration potential and gene expression profile of human mesenchymal stem cells induced by CCL25. Exp Cell Res 2009;315(8):1468–79.
[29] Ringe J, Strassburg S, Neumann K, Endres M, Notter M, Burmester GR, et al. Towards in situ tissue repair: human mesenchymal stem cells express chemokine receptors CXCR1, CXCR2 and CCR2, and migrate upon stimulation with CXCL8 but not CCL2. J Cell Biochem 2007;101(1):135–46.
[30] Gimble JM, Youkhana K, Hua X, Bass H, Medina K, Sullivan M, et al. Adipogenesis in a myeloid supporting bone marrow stromal cell line. J Cell Biochem 1992;50(1):73–82.
[31] Pittenger MF, Mackay AM, Beck SC, Jaiswal RK, Douglas R, Mosca JD, et al. Multilineage potential of adult human mesenchymal stem cells. Science 1999; 284(5411):143–7.
[32] Arbab AS, Yocum GT, Kalish H, Jordan EK, Anderson SA, Khakoo AY, et al. Efficient magnetic cell labeling with protamine sulfate complexed to ferumoxides for cellular MRI. Blood 2004;104(4):1217–23.
[33] Bulte JW, Douglas T, Witwer B, Zhang SC, Strable E, Lewis BK, et al. Magnetodendrimers allow endosomal magnetic labeling and in vivo tracking of stem cells. Nat Biotechnol 2001;19(12):1141–7.
[34] Arbab AS, Yocum GT, Wilson LB, Parwana A, Jordan EK, Kalish H, et al. Comparison of transfection agents in forming complexes with ferumoxides, cell labeling efficiency, and cellular viability. Mol Imaging 2004;3(1):24–32.
[35] Lewin M, Carlesso N, Tung CH, Tang XW, Cory D, Scadden DT, et al. Tat peptide-derivatized magnetic nanoparticles allow in vivo tracking and recovery of progenitor cells. Nat Biotechnol 2000;18(4):410–4.
[36] Josephson L, Tung CH, Moore A, Weissleder R. High-efficiency intracellular magnetic labeling with novel superparamagnetic-Tat peptide conjugates. Bioconjug Chem 1999;10(2):186–91.
[37] Zhang Y, Kohler N, Zhang M. Surface modification of superparamagnetic magnetite nanoparticles and their intracellular uptake. Biomaterials 2002; 23(7):1553–61.
[38] Bulte JW, Hoekstra Y, Kamman RL, Magin RL, Webb AG, Briggs RW, et al. Specific MR imaging of human lymphocytes by monoclonal antibody-guided dextran-magnetite particles. Magn Reson Med 1992;25(1):148–57.
[39] Gamarra LF, Pavon LF, Marti LC, Pontuschka WM, Mamani JB, Carneiro SM, et al. In vitro study of CD133 human stem cells labeled with superparamagnetic iron oxide nanoparticles. Nanomedicine 2008;4(4):330–9.
[40] Mailander V, Lorenz MR, Holzapfel V, Musyanovych A, Fuchs K, Wiesneth M, et al. Carboxylated superparamagnetic iron oxide particles label cells intracellularly without transfection agents. Mol Imaging Biol 2008;10(3):138–46.
[41] Matuszewski L, Persigehl T, Wall A, Schwindt W, Tombach B, Fobker M, et al. Cell tagging with clinically approved iron oxides: feasibility and effect of lipofection, particle size, and surface coating on labeling efficiency. Radiology 2005;235(1):155–61.
[42] Thorek DL, Tsourkas A. Size, charge and concentration dependent uptake of iron oxide particles by non-phagocytic cells. Biomaterials 2008;29(26):3583–90.
[43] Chithrani BD, Ghazani AA, Chan WC. Determining the size and shape dependence of gold nanoparticle uptake into mammalian cells. Nano Lett 2006;6(4):662–8.
[44] Schäfer R, Kehlbach R, Muller M, Bantleon R, Kluba T, Ayturan M, et al. Labeling of human mesenchymal stromal cells with superparamagnetic iron oxide leads to a decrease in migration capacity and colony formation ability. Cytotherapy 2009;11(1):68–78.
[45] Bulte JW, Kraitchman DL, Mackay AM, Pittenger MF. Chondrogenic differentiation of mesenchymal stem cells is inhibited after magnetic labeling with ferumoxides. Blood 2004;104(10):3410–2 [author reply 3412–3413].
[46] Kostura L, Kraitchman DL, Mackay AM, Pittenger MF, Bulte JW. Feridex labeling of mesenchymal stem cells inhibits chondrogenesis but not adipogenesis or osteogenesis. NMR Biomed 2004;17(7):513–7.
[47] Henning TD, Sutton EJ, Kim A, Golovko D, Horvai A, Ackerman L, et al. The influence of ferucarbotran on the chondrogenesis of human mesenchymal stem cells. Contrast Media Mol Imaging 2009;4(4):165–73.
[48] Lee ES, Chan J, Shuter B, Tan LG, Chong MS, Ramachandra DL, et al. Microgel iron oxide nanoparticles for tracking human fetal mesenchymal stem cells through magnetic resonance imaging. Stem Cells 2009;27(8):1921–31.
[49] Balakumaran A, Pawelczyk E, Ren J, Sworder B, Chaudhry A, Sabatino M, et al. Superparamagnetic iron oxide nanoparticles labeling of bone marrow stromal (mesenchymal) cells does not affect their "stemness". PLoS One 2010;5(7): e11462.

[50] Arbab AS, Yocum GT, Rad AM, Khakoo AY, Fellowes V, Read EJ, et al. Labeling of cells with ferumoxides-protamine sulfate complexes does not inhibit function or differentiation capacity of hematopoietic or mesenchymal stem cells. NMR Biomed 2005;18(8):553–9.
[51] Soenen SJ, Himmelreich U, Nuytten N, De Cuyper M. Cytotoxic effects of iron oxide nanoparticles and implications for safety in cell labelling. Biomaterials 2011;32(1):195–205.
[52] Nohroudi K, Arnhold S, Berhorn T, Addicks K, Hoehn M, Himmelreich U. In vivo MRI stem cell tracking requires balancing of detection limit and cell viability. Cell Transplant 2010;19(4):431–41.
[53] Cengelli F, Maysinger D, Tschudi-Monnet F, Montet X, Corot C, Petri-Fink A, et al. Interaction of functionalized superparamagnetic iron oxide nanoparticles with brain structures. J Pharmacol Exp Ther 2006;318(1):108–16.